 doi:10.20944/preprints202106.0405.v1

Article

Process analysis of main organic compounds dissolved in aqueous phase by hydrothermal processing of Açaí (*Euterpe Oleraceae*, Mart.) seeds: Influence of process temperature, biomass-to-water ratio, and production scales

Conceição de Maria Sales da Silva[3], Douglas Alberto Rocha de Castro[3], Marcelo Costa Santo[2], Hélio da Silva Almeida[2,3], Ulf Lüder[4], Maja Shultze[1]; Judi A. Libra[1]; Jan Mumme[1]; Thomas Hofmann[1], Nélio Teixeira Machado[1,2,3]*

[1] Leibnitz-Institüt für Agrartechnik Potsdam-Bornin e.V, Department of Postharvest Technology, Max-Eyth-Alee 100, Potsdam 14469, Germany; atb@atb-potsdam.de
[2] Faculty of Sanitary and Environmental Engineering, Rua Corrêa N° 1, Campus Profissional-UFPA, Belém-Pará-Brazil, CEP: 66075-900; faesa@ufpa.br
[3] Graduate Program of Natural Resources Engineering of Amazon; Rua Corrêa N° 1, Campus Profissional-UFPA, Belém-Pará-Brazil, CEP: 66075-110, proderna@ufpa.br
[4] SunCoal Industries GmbH, Rudolf-Diesel-Straße 15, 14974 Ludwigsfelde, Germany, info@suncoal.com
* Correspondence: machado@ufpa.br; Tel.: +55-91-984620325

Abstract: This work aims to investigate systematically the influence of process temperature, biomass-to-water ratio, and production scales (laboratory and pilot) on the chemical composition of aqueous and gaseous phases and *mass production of chemical* by hydrothermal processing of Açaí (*Euterpe Oleraceae*, Mart.) seeds. The hydrothermal carbonization carried out at 175, 200, 225, and 250 °C, 2 °C/min, biomass-to-water ratio of 1:10, and at 250 °C, 2 °C/min, and biomass-to-water ratios of 1:10, 1:15, and 1:20, in technical scale, as well as at 200, 225, and 250 °C, 2 °C/min, biomass-to-water ratio of 1:10, in laboratory scale. The elemental composition (C, H, N, S) of solid phase determined to compute the HHV. The chemical composition of aqueous phase determined by GC and HPLC and the volumetric composition of gaseous phase by using an infrared gas analyzer. For the experiments in pilot scale with constant biomass-to-water ratio of 1:10, the yields of solid, liquid, and gaseous phases varied between 53.39 and 37.01% (wt.), 46.61 and 59.19% (wt.), and 0.00 and 3.80% (wt.), respectively. The yield of solids shows a smooth exponential decay with temperature, while that of liquid and gaseous phases a smooth growth. By varying the biomass-to-water ratios, the yields of solid, liquid, and gaseous reaction products varied between 53.39 and 32.09% (wt.), 46.61 and 67.28% (wt.), and 0.00 and 0.634% (wt.), respectively. The yield of solids decreases exponentially with increasing water-to-biomass ratio and that of liquid phase increases in a sigmoid fashion. For constant biomass-to-water ratio, the concentrations of Furfural and HMF decrease drastically with increasing temperature, reaching a minimum at 250 °C, while that of phenols increases. In addition, the concentrations of CH_3COOH and total carboxylic acids increase, reaching a maximum at 250 °C. For constant process temperature, the concentrations of aromatics vary smoothly with the temperature. The concentrations of furfural, HMF, and cathecol decrease with temperature, while that of phenols increases. The concentrations of CH_3COOH and total carboxylic acids decrease exponentially with temperature. Finally, for the experiments with varying water-to-biomass ratios, the productions of chemicals (furfural, HMF, phenols, cathecol, and acetic acid) in the aqueous phase is highly dependent on the biomass-to-water ratio. *For the experiments in laboratory scale with constant biomass-to-water ratio of 1:10, the yields of solid ranged between 55.9 and 51.1% (wt.), showing not only a linear decay with temperature, but also a lower degradation grade. The chemical composition of main organic compounds (furfural, HMF, phenols, cathecol, and acetic acid) dissolved in the aqueous phase in laboratory scale shows the same behavior of those in obtained in pilot scale.*

Keywords: Açaí seeds; hydrothermal carbonization; hot compressed water; process analysis, HMF, Furfural, Acetic Acid, Mass Production.

Preprints (www.preprints.org) | NOT PEER-REVIEWED | Posted: 15 June 2021 doi:10.20944/preprints202106.0405.v1

1. Introduction

Açaí (*Euterpe oleracea* Mart.) is palm native to the Brazilian Amazon [1]. It has abundant occurrence in the Amazon estuary floodplains [2-3]. The Açaí fruits *in nature* have a great economic importance for the agroindustry, as well as extractive activities of rural communities of the Brazilian Amazonian state of Pará [4]. The fruit is a small dark-purple, berry-like fruit, almost spherical, weighing between 2.6 to 3.0 g [5]. It has a diameter around 10.0 and 20.0 mm [5], containing a large core seed/kernel that occupies between 85-95% (vol./vol.) of its volume [3,6].

By processing/extracting the pulp and skin with warm water to produce a thick, purple-colored juice [3, 6], a waste is generated [7-11], the Açaí seeds, a rich lignin-cellulosic residue with great potential to energetic use [8-9, 12]. In the crop years 2016-2017 around 1200-1274 million tons of Açaí fruits were produced in Brazil, being the state of Pará the main producer (94%), generating large amounts of solid residues, consisting of seeds and fibers [4-9].

The residue of Açaí fruits (seeds + fibers) processing has a fibrous outer layer, containing 46.51% (wt.) cellulose and 30.31% (wt.) lignin [11], being the residue (seeds + fibers) composed by 36.13% (wt.) cellulose, 47.92% (wt.) lignin, 1.57% (wt.) ash, and 16.64% (wt.) extractives [11], representing an important biomass renewable source for energetic applications [8-9, 12].

The thermo-chemical transformation of lignin-cellulose rich biomass with H_2O in the sub-critical or supercritical state is a promising technique, and the literature reports several studies on the subject [13-46]. *Li et. all.* [13], applied statistical methods to investigate the role of process conditions (temperature, reaction time, biomass-to-water ratio) and chemical raw material characteristics on the physical-chemistry properties hydrothermal carbonization products (solid, liquid, and gas). In addition, *Li et. all.* [13], reported that most commonly cited hydrothermal carbonization product parameter was solid (hydrochar) yield (71%), while little attention has been paid to carbon-related information to the liquid and gaseous phases (< 18%), *which includes the analysis of chemical composition*.

In fact, only a few studies investigated systematically the composition of main chemical compounds, such as aromatic-ring compounds (*Furfural*, *HMF*, *Phenols*, *Cresols, Cathecol*, *Guaiacol, etc.*) [14, 18, 39-41], carboxylic acids (*HCOOH*, *CH_3COOH*, *CH_3CH_2COOH*, *$CH_3CH(OH)COOH$*, *$CH_3C(O)CH_2CH_2COOH$, etc.*) [14, 18, 39-40, 43], alcohols (*CH_3OH*, *CH_3CH_2OH*) [14], sugars (*Glucose*, *Xylose*, *Galactose*, *Fructose, Sucrose, Mannosan*, *Levoglucosan*, etc.) [18, 40, 43], and BTEX (*Benzene, Toluene*, *Xylenes*, and *Ethyl benzene*) [41], dissolved in the process water by hydrothermal carbonization of biomass, including the hydrothermal processing of corn Stover [14, 18], Tahoe mix, Pinyon/Juniper, and Loblolly pine wood, sugar bagasse, and rice hulls [18], wheat straw, wheat straw digestate, Poplar, Garapa, massaranduba, and pine wood, α-Cellulose, and D-(+)-xylose [39], wheat straw, Poplar, and α-Cellulose [40], wheat straw, wheat straw digestate, Poplar, Garapa, massaranduba, and pine wood [41], and Tahoe mix [43]. Recently, *Poerschmann et. all.* [44], investigated the distribution of main medium molar mass compounds dissolved in process water by hydrothermal carbonization of glucose, fructose and xylose by GC-MS and IC, identifying more than 50 compounds, being the most abundant carboxylic acids (formic, acetic, glycolic, lactic, and levulinic acids) and aromatic-ring compounds (Furfural, 5-(Hydroxymethyl)-2-furfural).

Another process parameter affecting the physical-chemistry properties hydrothermal carbonization products (solid, liquid, and gas) is the water-to-biomass ratio [19, 25-30]. In the last years only a few studies investigated the influence of water-to-biomass ratio by hydrothermal processing of biomass, including *tomato-pell-waste* [26], *olive stone* [27], *microalgae* [28], *sawdust* [29], *banana peels* [30], *wood ships* [25], and *corn Stalk* [19], but no study has examined it´s influence consistently [13], particularly the composition of main chemical compounds dissolved in the process water.

Açaí (*Euterpe oleracea*, Mart.) seed is the only fruit specie, whose centesimal and elemental composition is completely different from wood biomass (Poplar, Garapa, massa-

Preprints (www.preprints.org) | NOT PEER-REVIEWED | Posted: 15 June 2021 doi:10.20944/preprints202106.0405.v1

randuba, Tahoe mix, Pinyon/Juniper, Loblolly pine, and pine wood) [18, 39-41, 43], agriculture residues of cereal grains (corn Stover, corn Stalk, rice hulls, wheat straw), agriculture residues of sugar cane (sugar bagasse) [18]. Although, hydrothermal treatment has been applied to enhance enzymatic hydrolysis of Açaí seeds in aqueous-H_2SO_4 at 121 °C [47], *until the moment no systematic study investigated the influence of temperature, biomass-to-water ratio, and production scales (laboratory and pilot) on the chemical composition of aqueous and gaseous phases, as well as on the mass production of chemicals by hydrothermal carbonization of Açaí seeds in technical scale*.

This work aims to investigate the influence of process temperature, biomass-to-water ratio, and production scales (laboratory and pilot) on the chemical composition of main chemical compounds, such as aromatic-ring compounds, carboxylic acids, and alcohols, dissolved in process water, the gaseous phase composition, and mass production of chemicals by hydrothermal processing of Açaí (*Euterpe Oleraceae*, Mart.) seeds in technical scale.

2. Materials and Methods

2.1. Methodology

The process flow sheet shown in Figure 1 summarizes the applied methodology, described in a logical sequence of ideas, chemical methods, and procedures to analyze the the chemical composition of main compounds in the liquid phase by HTC of Açaí seeds.

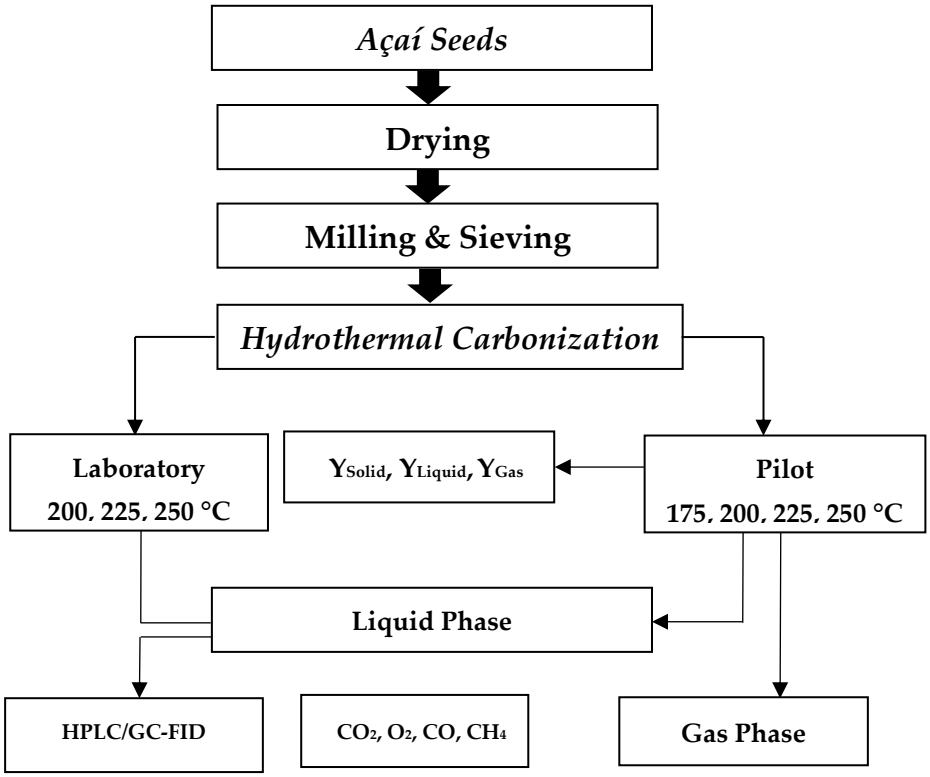

Figure 1. Process flow sheet by the production of fuel-like fractions (gasoline, light kerosene, and kerosene) obtained by fractional distillation of bio-oil obtained in laboratory, bench, and pilot scales.

Initially, the Açaí seeds are collected. Afterwards, subjected to pre-treatments of drying, followed by milling and sieving. The HTC carried out in laboratory and pilot scales to investigate the influence of temperature (175, 200, 225, 250 °C) and biomass-to-water ratio (1:10, 1:15, 1:20) on the yields of hydro-char, H_2O, and gas, as well as on the chemical composition in the liquid phase. Finally, the influence of production scales on the composition of main compounds (*Furfural*, *HMF*, *Phenols*, *Cathecol*, *Guaiacol*, *HCOOH*, *etc.*) in the liquid phase investigated. The composition in the gas phase (CH_4, CO_2, O_2, CO) determined by infrared spectroscopy, and that of liquid by HPLC and GC-FID.

Preprints (www.preprints.org) | NOT PEER-REVIEWED | Posted: 15 June 2021 doi:10.20944/preprints202106.0405.v1

2.2. *Materials, pre-treatment, and characterization of Açaí seeds in nature*

The charges of Açaí seeds *in nature* obtained in a small store of Açaí in the City of Belém-Pará-Brazil [12]. The seeds dried at 105 °C, grinded using a knife cutting mill, and sieved using an 18 Mesh sieve [12]. Afterwards, the seeds were physical-chemistry characterized for moisture (AOAC 935.29), volatile matter (ASTM D 3175-07), ash (ASTM D 3174-04), fixed carbon (ASTM D6316-09), lipids (AOAC 963.15), proteins (AOAC 991.20) [12], fibers according to the literature [48], and insoluble lignin by the modified method of Klason [49]. The elemental composition (C, H, N, S) of Açaí seeds and solid phase determined. Figure 2 shows the Açaí seeds after drying, milling and sieving [Seeds + Fibers (a); Comminuted Seeds + Fibers (b); and Sieved Seeds + Fibers (c)]. HTC experiments carried out with sieved seeds + fibers, as shown in Figure 2 (c).

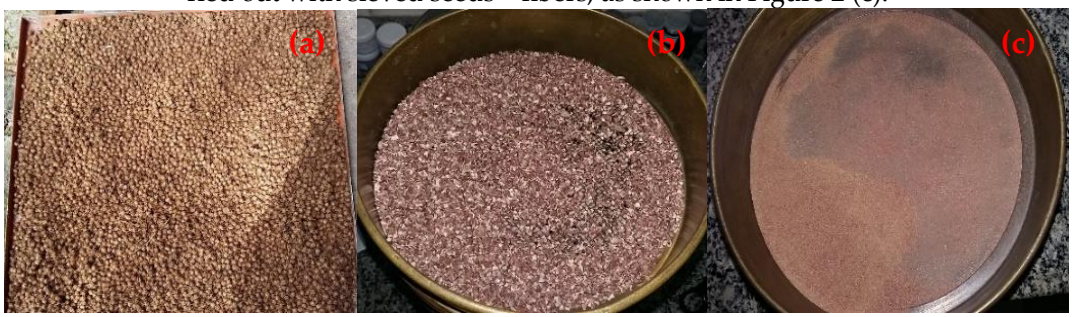

Figure 2. Material after drying, milling and sieving process of Açaí seeds [Seeds + Fibers (a); Comminuted Seeds + Fibers (b); and Sieved Seeds (c)].

2.3. *Experimental apparatus and procedures*

2.3.1. Experimental apparatus and procedures in pilot scale

Pilot scale apparatus illustrated in Figure 3, described in details elsewhere [14].

Figure 3. Pilot scale stirred tank stainless steel reactor of 18.925 L (Parr, USA, Model: 4555).

The hydrothermal processing of dried Açaí seeds carried out with hot compressed at 175, 200, 225, and 250 °C, 240 minutes, biomass-to-water ratio of 1:10, and at 250 °C, 240 minutes, and biomass-to-water ratios of 1:10, 1:15, and 1:20, as described in details elsewhere [14].

2.3.2. Experimental apparatus and procedures in laboratory scale

Preprints (www.preprints.org) | NOT PEER-REVIEWED | Posted: 15 June 2021 doi:10.20944/preprints202106.0405.v1

The laboratory scale apparatus illustrated in Figure 4. The laboratory scale cylindrical stirred tank stainless steel reactor of 1.0 L (Parr, USA, Model: 4577), with internal diameter of 9.525 cm and 15.748 cm, weights 7.257 kg. The reactor contains a mechanical agitation system with a stirrer motor of ¼ hp, 1.81 N.m Torque, and 02 impellers (ID=5.08 cm) with 6-blades, a ceramic movable heater of 2800 W, a modular controller (Parr, USA, Model: 4848), 02 type J thermocouples inside a thermos well, operates at maximum 345 bar and 500 °C. The hydrothermal processing of dried Açaí seeds carried out with hot compressed at 200, 225, and 250 °C, 240 minutes, biomass-to-water ratio of 1:10. Initially, the solid moisture determined and the mass of water computed based on the dried solid. 73.50 g of solid with 25% (wt.) moisture added to 532.82 g of distilled and deionized water introduced in the reactor. The operating temperatures (200, 225, and 250 °C) set for a heating rate of 2.0 °C/min. The reaction time computed from the time the reactor reaches the set point temperature (τ_0). Afterwards, the reactor cooled down until ambient temperature. The reaction products, a moist dewatered solid phase and a liquid phase, determined gravimetrically. Then, the moist solid phase dried at 105 °C for 24 h. The volume of gas and its composition determined, as described elsewhere [14]. The Samples of moist dewatered solids, liquid phase, and dried solid phase stored for physicochemical analysis.

Figure 4. Pilot scale stirred tank stainless steel reactor of 1.0 L (Parr, USA, Model: 4577).

2.4. Compositional analysis of reaction products

2.4.1. Aqueous phase

The chemical analysis of volatile low-chain length carboxylic acids (R-COOH, with R_1=CH_3, R_2=C_2H_5, R_3=C_3H_7, R_4=C_4H_9) and alcohols (R-OH, with R_1=CH_3, R_2=C_2H_5, R_3=C_3H_8), selective cellulose/hemicellulose-derived compounds by hydrothermal processing of biomass, identified by GC while the selective cellulose/hemicellulose-derived phenolic (phenol, cresol, catechol, and guaiacol) and aldehydes (Furfural, HMF) compounds identified by HPLC. The equipment specifications (GC, HPLC) and operating conditions described in details elsewhere [14].

2.4.2. Gaseous phase

The volume of gas, degassed at 25 °C and 1.0 atmosphere, measured with a gas flow meter, while an infrared gas analyzer used to determine the volumetric composition of gaseous products [14]. The equipment's specifications and procedures described in details elsewhere [14].

2.5. Steady state material balance by hydrothermal carbonization

Preprints (www.preprints.org) | NOT PEER-REVIEWED | Posted: 15 June 2021 doi:10.20944/preprints202106.0405.v1

The yields of reaction products (solid, liquid, and gaseous phases) were determined by applying the mass conservation principle within the stirred tank reactor, operating in batch mode, closed thermodynamic system, and the equations described in details elsewhere [14].

3. Results

3.1. Hydrothermal processing of Açaí seeds

3.1.1. Material balances, operating conditions, and yields of reaction products

3.1.1.1. Influence of temperature on the yields of reaction products

The material balances, operating conditions, and yields of reaction products by hydrothermal processing of Açaí seeds *in nature* at *175, 200, 225, 250* °C, 2 °C/min, 240 min, and biomass-to-water ratio of 1:10, in pilot scale, are summarized in Table 1.

Table 1. Mass balances, process and operating conditions, and yields of solid, liquid, and gaseous products by hydrothermal processing of Açaí seeds with hot compressed H_20 at *175, 200, 225, 250* °C, 2 °C/min, 240 min, and biomass-to-water ratio of 1:10, in pilot scale.

	Temperature [°C]			
Process Parameters	**175**	**200**	**225**	**250**
Mass of Açaí Seeds [g]	**300.00**	**299.82**	**299.98**	**300.16**
Mass of H_2O [g]	**2997.60**	**3000.20**	**3001.30**	**2999.90**
Mechanical Stirrer Speed [rpm]	90	90	90	90
Initial Temperature [°C]	30	30	30	30
Heating Rate [°C/min]	2	2	2	2
Process Time [min]	240	240	240	240
Mass of Slurry [g]	**3252.20**	**3240.20**	**3216.50**	**3167.40**
Volume of Gas [mL], T = 25 °C, P = 1 atm	**0**	**5290**	**5590**	**7470**
Mass of Gas [g]	**0**	**7.564**	**8.231**	**11.408**
Process Loss (I) [g]	**45.40**	**59.82**	**84.78**	**132.66**
Input Mass of Slurry (Pressing) [g]	3252.20	3240.20	3216.50	3161.70
Process Loss (II) [g]	**0.00**	**0.00**	**0.00**	**5.70**
Mass of Liquid Phase [g]	2638.53	2615.56	2637.97	2556.96
Mass of Moist Hydro-char [g]	588.10	587.37	557.61	591.29
Process Loss (III) [g]	**25.57**	**37.27**	**20.92**	**13.41**
Mass of Dry Hydro-char [g]	**160.16**	**118.53**	**113.052**	**111.092**
(Mass of Liquid Phase + Σ Process Loss + Mass of Moist Hydro-char - Mass of Dry Hydro-char - Mass of Gas) [g]	3137.44	3173.926	3179.997	3177.52
Process Loss (I + II + III) [g]	**70.97**	**97.09**	**105.70**	**151.77**
Mass of $Liquid_{Reaction}$ [g]	139.84	173.726	178.697	177.62
Yield of Hydro-char [wt.%]	**53.39**	**39.534**	**37.686**	**37.011**
Yield of Liquid Phase [wt.%]	**46.61**	**57.943**	**59.570**	**59.188**
Yield of Gas [wt.%]	**0.000**	**2.523**	**2.744**	**3.801**

Figure 5 shows the effect of temperature on the yields of reaction products by hydrothermal processing of Açaí seeds *in nature* with hot compressed H_20 at *175, 200, 225, 250* °C, 2 °C/min, 240 min, and biomass-to-water ratio of 1:10. The exponential function applied to regress the yields of reaction products, correlating well the experimental data for both the solid and liquid phases, with r^2 (R-Squared) between 0.996 and 0.996. The yield of solids shows a smooth first-order exponential decay behavior, while that of liquid and gaseous phases a smooth first-order exponential growth. At 175 °C hydrothermal carbonization takes places, as the main reaction product is a solid [15]. From 200 °C, hydrothermal liquefaction occurs, as the maim reaction products are liquids [15]. The hydro-char yields are according to those reported in the literature for *Rye straw* [16], *Eucalyptus leaves* [17], *corn Stover* [14], *Sugarcane bagasse* [18]; and *corn Stalk* [19].

Preprints (www.preprints.org) | NOT PEER-REVIEWED | Posted: 15 June 2021 doi:10.20944/preprints202106.0405.v1

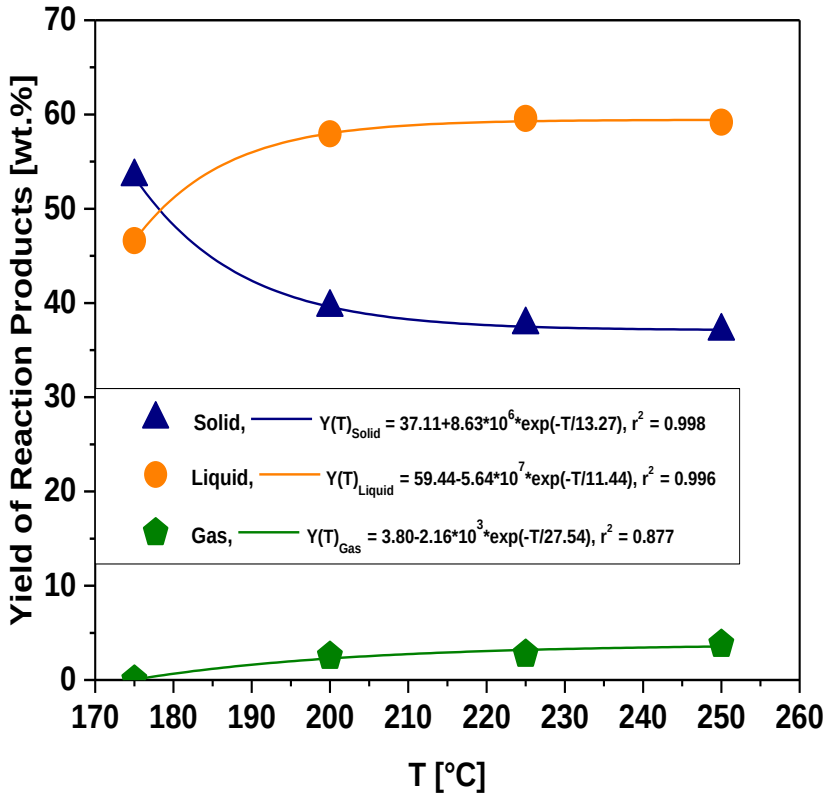

Figure 5. Effect of temperature on the yields of reaction products by hydrothermal processing of Açaí seeds *in nature*.

The centesimal composition of Açaí (*Euterpe oleracea* Mart.) seeds [12], shows 40.29% (wt.) cellulose, 5.5% (wt.) hemi-cellulose, 4.0% (wt.) lignin, ***29.79% fibers***, as well as 6.25% (wt.) proteins, 0.61% (wt.) lipids, 10.15% (wt.) moisture, 0.5% (wt.) volatile matter, 0.83% (wt.) fixed carbon, and 0.15% (wt.) ash. The centesimal composition of Açaí fibers *in nature*, shows 41.37% (wt.) cellulose, 11.54% (wt.) hemi-cellulose, 40.25% (wt.) lignin, 1.96% ash, and 8.88% moisture, as reported by *Tavares et. all.* [7].

Based on the fact that 61.25% (wt.) cellulose and 15% (wt.) lignin decompose by 200 °C, 24 hours, 1:10 biomass-to-water ratio, according to *Falco et. all.* [16], that 5.0% (wt.) lipids and 72% (wt.) proteins decompose at 350 °C, 90 min, 1:5.7 biomass-to-water ratio, as reported by *Teri et. all.* [20], that hemicellulose degrades 65% (wt.) by severity factor between 4.5 and 5.0, as reported by *Borrero-López et. all.* [21], and that approximately 50% (wt.) cotton fibers decompose at 210 °C, 8.0 hours, 1:41 biomass-to-water ratio, as reported by *Zhang et. all.* [22], one may perform a centesimal mass balance to compute the approximate theoretical mass degradation of Açaí seeds at 200 °C, 2 °C/min, 240 min, and biomass-to-water ratio of 1:10, using the equation as follows, computed in Table 2. The $Y_{Hydro\text{-}char/Cellulose}$ computed by multiplying the percentage of cellulose in the centesimal composition of Açaí seeds by the fraction of non-degraded cellulose ($Y_{Hydro\text{-}char/Cellulose}$ = 40.29%*(100-61.25)/100 = 15.6124%), as summarized in Table 2.

$$Y_{Hydro\text{-}char} = \sum Y_{Hydro\text{-}char/Cellulose} + Y_{Hydro\text{-}char/Lignin} + Y_{Hydro\text{-}char/Hemi\text{-}Cellulose} + Y_{Hydro\text{-}char/Proteins} + Y_{Hydro\text{-}char/Lipids} + Y_{Hydro\text{-}char/Fibers} \quad (1)$$

The yield of hydro-char is very close to the experimental value of 39.534% (wt.), showing a deviation of 2.51%, if the yield of $Y_{Hydro\text{-}char/Fibers}$ is computed based on the decomposition of cellulose, lignin, and hemi-cellulose ($Y_{Hydro\text{-}char/Fibers}$ = 16.17%), and 5.68%, if the yield of $Y_{Hydro\text{-}char/Fibers}$ is computed based on the decomposition of fibers ($Y_{Hydro\text{-}char/Fibers}$ = 14.895%). In addition, the computed amount of Açaí seeds fibers [29.79% (wt.)] degraded

Preprints (www.preprints.org) | NOT PEER-REVIEWED | Posted: 15 June 2021 doi:10.20944/preprints202106.0405.v1

at 200 °C, 240 min, and biomass-to-water ratio of 1:10 was 16.17% (wt.), giving a degradation percentage 54.28%, very close to the results reported by *Zhang et. all.* [22], who stated that approximately 50% (wt.) cotton fibers decompose at 210 °C, 8.0 hours, 1:41 biomass-to-water ratio.

Table 2. Computation of hydro-char yield. Centesimal composition of Açaí seeds and Açaí fibers *in nature* [7, 12], decomposition cellulose and lignin [16], decomposition of lipids and proteins [20], decomposition of hemicellulose [21], decomposition of cotton fibers [22].

		Decomposition					
Centesimal composition	**[wt.%]**	**Cellulose** [wt.%]	**Lignin** [wt.%]	**Hemi-cellulose** [wt.%]	**Proteins** [wt.%]	**Lipids** [wt.%]	**Fibers** [wt.%]
		61.25	**15.00**	**65.00**	**72.00**	**5.00**	**50.00**
Açaí Seeds [12]							
Cellulose	40.29	**15.6124**					
Lignin	4.00		**3.40**				
Hemi-cellulose	5.50			**1.925**			
Proteins	6.25				**1.82**		
Lipids	0.61					**0.5795**	
Fibers	29.79						**14.895**
Moisture	10.15						
Volatile matter	0.50						
Fixed carbon	0.83						
Ash	0.15						
$Y_{Hydro\text{-}char/Seeds}$ [wt.%]	**37.287**	**15.6124**	**3.400**	**1.925**	**1.820**	**0.5795**	**14.895**
Açaí Fibers [7]							
Cellulose	41.37	**16.080**					
Lignin	40.25		**34.213**				
Hemi-cellulose	11.54			**4.039**			
Moisture	8.88						
Ash	1.96						
$Y_{Hydro\text{-}char/Fibers}$ [wt.%]	**16.170**	**4.775**	**10.192**	**1.203**			

By analyzing the thermal decomposition behavior of cellulose and lignin reported by *Falco et. all.* [16], one observes that decomposition of cellulose is almost constant between 200 °C and 240 °C (38.75→37.00), showing that degradation/de-polymerization of cellulose is less intense [19], while lignin loses only 7.5% its initial mass (85%→77.5%), thus making it possible to explain the small differences for the solid phase yields between 200 °C and 250 °C.

The material balances, operating conditions, and yields of reaction products by hydrothermal processing of Açaí seeds *in nature* at *200, 225, 250* °C, 2 °C/min, 240 min, and biomass-to-water ratio of 1:10, in laboratory scale, are summarized in Table 3.

Figure 6 makes a comparison for the yields of solid phase products as a function of temperature by hydrothermal processing of Açaí seeds *in nature* with hot compressed H_20 at *175, 200, 225, 250* °C, 2 °C/min, 240 min, and biomass-to-water ratio of 1:10, in laboratory and pilot scales. One observes, for the temperature interval 200-250 °C, the yield of solid phase products varied between 39.53 and 37.01% (wt.) in pilot scale, while that in laboratory varied between 41.86 and 38.31% (wt.), showing deviations between 5,56 and 3,39%. *The yield of solid phase products in laboratory and pilot scale are very close, showing that production scales had little effect on hydro-char yield.* A linear function applied to regress the yield of hydro-char in laboratory scale, correlating very well the experimental data, with r^2 (R-Squared) of 0.999.

Table 3. Mass balances, process and operating conditions, and yields of solid, liquid, and gaseous products by hydrothermal processing of Açaí seeds with hot compressed H_20 at *200, 225, 250* °C, 2 °C/min, 240 min, and biomass-to-water ratio of 1:10, in laboratory scale.

	Temperature [°C]		
Process Parameters	**200**	**225**	**250**
Mass of Açaí Seeds [g]	**73.50**	**73.50**	**73.50**
Moist Content of Açaí Seeds [wt.%]	**25.23**	**25.23**	**25.23**
Mass of H_2O in Açaí Seeds [g]	*18.54*	*18.54*	*18.54*

Preprints (www.preprints.org) | NOT PEER-REVIEWED | Posted: 15 June 2021 doi:10.20944/preprints202106.0405.v1

Mass of H_2O [g]	**531.01**	**531.01**	**531.01**
Mechanical Stirrer Speed [rpm]	90	90	90
Initial Temperature [°C]	30	30	30
Heating Rate [°C/min]	2	2	2
Process Time [min]	240	240	240
Volume of Gas [mL], T = 25 °C, P = 1 atm	**1395**	**2475**	**3215**
CO_2 [vol.%]	**48.60**	**44.80**	**35.80**
CH_4 [vol.%]	**1.90**	**1.20**	**0.60**
O_2 [vol.%]	**9.20**	**9.90**	**12.10**
100 - Σ (CO_2 + CH_4 + O_2) [vol.%]	**40.30**	**44.10**	**51.50**
Mass of Gas [g]	**1.94**	**3.57**	**4.70**
Mass of Dry Hydro-char [g]	**30.77**	**29.43**	**28.16**
Mass of $Liquid_{Reaction}$ [g]	34.72	36.01	36.59
Yield of Hydro-char [wt.%]	**41.86**	**40.04**	**38.31**
Yield of Liquid Phase [wt.%]	**47.24**	**48.99**	**49.78**
Yield of Gas [wt.%]	**2.64**	**4.86**	**6.39**

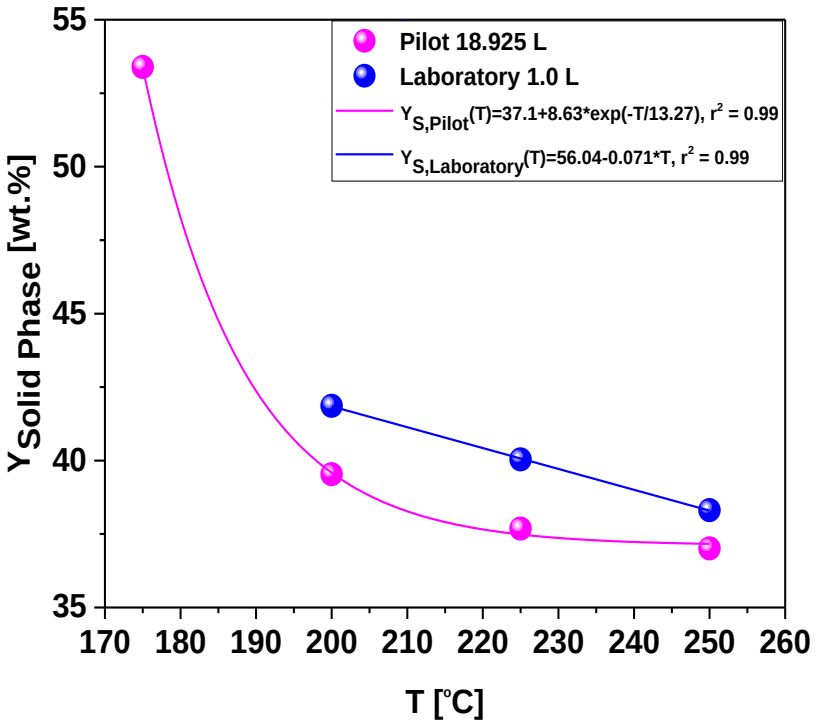

Figure 6. Influence of temperature on the solid phase yield by hydrothermal processing of Açaí seeds *in nature*, in laboratory and pilot scales.

3.1.1.2. Influence of biomass-to-water ratio on the yields of reaction products

Table 4 describes in details the material balances, operating conditions, and yields of reaction products by hydrothermal processing of Açaí seeds *in nature* at 250 °C, 2 °C/min, 240 min, and biomass-to-water ratios of 1:10, 1:15, and 1:20, in pilot scale.

Table 4. Mass balances, process and operating conditions, and yields of solid, liquid, and gaseous phases by hydrothermal processing of Açaí seeds with hot compressed H_20 at 250 °C, 2 °C/min, 240 min, and biomass-to-water ratios of 1:10, 1:15, and 1:20, in pilot scale.

	250 °C		
	Biomass/H_20 [-]		
Process Parameters	**1:10**	**1:15**	**1:20**
Mass of Açaí Seeds [g]	**300.16**	**300.28**	**300.07**
Mass of H_2O [g]	**2999.90**	**4502.90**	**6000.80**
Mechanical Stirrer Speed [rpm]	90	90	90
Initial Temperature [°C]	30	30	30
Heating Rate [°C/min]	2	2	2
Process Time [min]	240	240	240

Preprints (www.preprints.org) | NOT PEER-REVIEWED | Posted: 15 June 2021 doi:10.20944/preprints202106.0405.v1

Mass of Slurry [g]	**3167.40**	**4696.50**	**6217.40**
Volume of Gas [mL], T = 25 °C, P = 1 atm	**7470**	**1240**	**1225**
Mass of Gas [g]	**11.408**	**1.905**	**1.863**
Process Loss (I) [g]	**132.66**	**106.68**	**83.47**
Input Mass of Slurry (Pressing) [g]	3161.70	4696.50	6209.30
Process Loss (II) [g]	**5.70**	**0.00**	**8.10**
Mass of Liquid Phase [g]	2556.96	4077.05	5663.60
Mass of Moist Hydro-char [g]	591.29	585.83	518.45
Process Loss (III) [g]	**13.41**	**33.62**	**35.35**
Mass of Dry Hydro-char [g]	**111.092**	**102.25**	**96.302**
(Mass of Liquid Phase + Σ Process Loss + Mass of Moist Hydro-char - Mass of Dry Hydro-char - Mass of Gas) [g]	3177.52	5000.795	6210.805
Process Loss (I + II + III) [g]	**151.77**	**140.30**	**126.92**
Mass of $Liquid_{Reaction}$ [g]	177.62	196.125	202.535
Yield of Hydro-char [wt.%]	**37.011**	**34.051**	**32.093**
Yield of Liquid Phase [wt.%]	**59.188**	**65.315**	**67.286**
Yield of Gas [wt.%]	**3.801**	**0.634**	**0.621**

The effect of H_20-to-Biomass ratio on the yields of reaction products (solid, liquid, and gas) by hydrothermal of Açaí seeds *in nature*, illustrated in Figure 7 and comparison of hydro-char yields with similar data reported in the literature, shown in Figure 8. At 250 °C hydrothermal liquefaction is dominant, as the main reaction products formed are liquids [15]. The yields of reaction products, illustrated in Figure 7, were regressed using a dose-response function, showing r^2 (R-Squared) between 0.97 and 0.99. The yields of hydro-char and gas decrease with H_20-to-water ratios, while that of liquid phase increases. By increasing the H_20-to-Biomass ratio, the amount of reaction media (hot compressed H_20) increases, increasing the number of hydroxonium ion (H_3O^+) and a hydroxide ion (OH^-) dissociated within the reaction system, thus improving the catalyzes of chemical reactions such as hydrolysis and organic compounds degradation (e.g. depolymerization, fragmentation) without aid a catalyst [23]. In fact, according to the literature [24-25], increasing the H_20-to-Biomass ratio causes a great impact on hydrolysis reactions by hydrothermal processing of biomass.

A compilation of similar data on the effect of H_20-to-Biomass ratio over hydro-char yields illustrated in Figure 8. The behavior of hydro-char yields is similar, showing a decrease on the hydro-char yields as the H_20-to-Biomass ratio increases. The data for *Açaí seeds*, *tomato-pell-waste* [26], *olive stone* [27], and *corn Stalk* [19], were regressed using a dose-response function, showing r^2 (R-Squared) between 0.941 and 0.969. The experimental data are not only according to similar data reported in the literature for *tomato-pell-waste* [26], *olive stone* [27], *microalgae* [28], *sawdust* [29]; *banana peels* [30], *wood ships* [25], but close to that of *corn Stalk* [19], carried out at 250 °C and 4.0 h.

By analyzing Figure 8, one observes that temperature has a combined effect on the hydro-char yield with varying H_20-to-Biomass ratios. At higher temperatures (250 °C), the effect of H_20-to-Biomass is more intense, playing an important role on hydro-char yield. For low-medium hydrothermal processing temperatures, the effect of H_20-to-Biomass on hydro-char yield is secondary, as reported by [26].

Preprints (www.preprints.org) | NOT PEER-REVIEWED | Posted: 15 June 2021 doi:10.20944/preprints202106.0405.v1

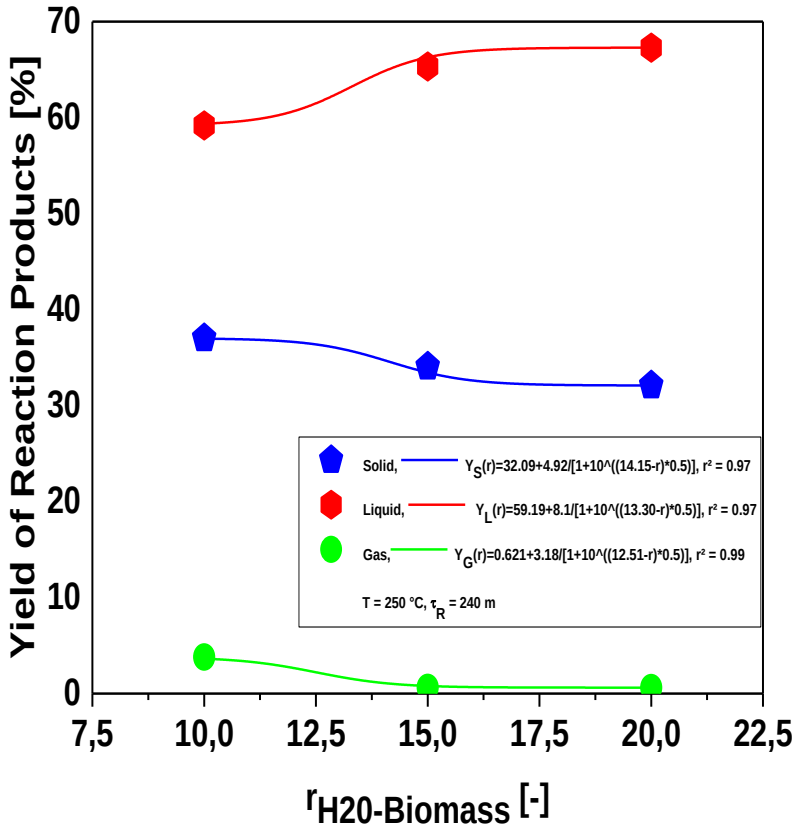

Figure 7. Effect of H20-to-Biomass ratio on the yields of reaction products.

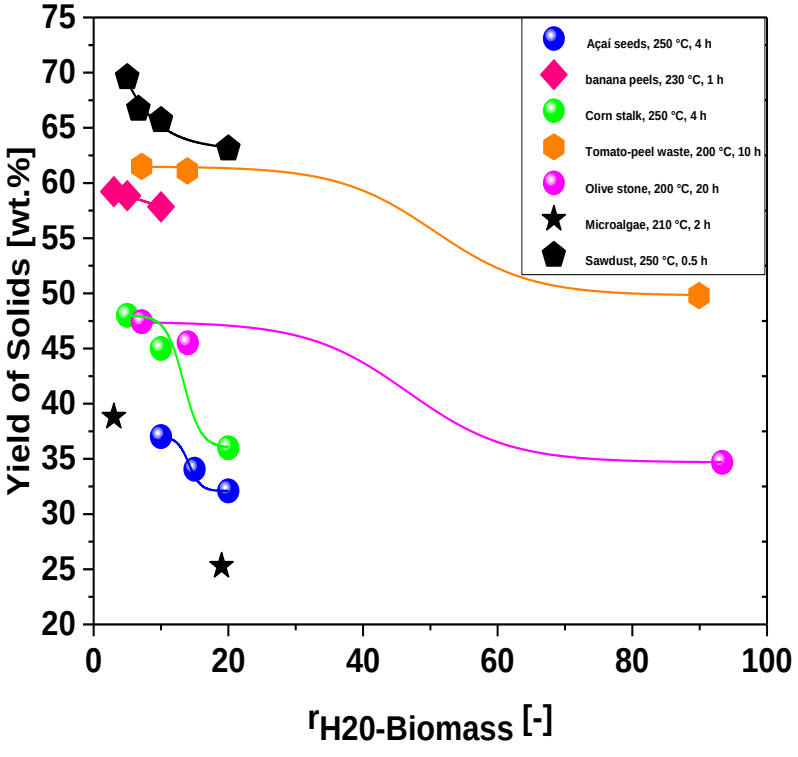

Figure 8. Comparison of hydro-char yield with similar data in the literature [19, 26-29].

3.1.2.Chemical composition of gas reaction products

Preprints (www.preprints.org) | NOT PEER-REVIEWED | Posted: 15 June 2021 doi:10.20944/preprints202106.0405.v1

3.1.2.1. Influence of temperature on the chemical composition of gas reaction products

The volume of gas degassed at 25 °C and 1.0 atmosphere by hydrothermal processing of Açaí seeds with hot compressed H_20 at *175, 200, 225, 250* °C, 2 °C/min, 240 min, and biomass-to-water ratio of 1:10, in pilot scale, is shown in Table 5.

Table 5. Volume of gas and composition of gas products at 25 °C and 1.0 atmosphere by hydrothermal processing of Açaí seeds with hot compressed H_20 at *175, 200, 225, 250* °C, 2 °C/min, 240 min, and biomass-to-water ratio of 1:10, in pilot scale.

	Temperature [°C]			
Composition [vol.%]	**175**	**200**	**200**	**200**
CO_2 [vol.%]	0.00	44.40	51.30	60.60
CH_4 [vol.%]	0.00	0.40	0.50	1.30
O_2 [vol.%]	0.00	1.0	0.30	0.00
100 - Σ (CO_2 + CH_4 + O_2) [vol.%]	0.00	54.20	47.90	38.10
Volume of Gas [mL]	**0.00**	**5290**	**5590**	**7470**
Volume of CO_2 [mL]	0.00	2348.76	2867.67	4526.82
Volume of CH_4 [mL]	0.00	21.16	27.95	97.11
Volume of O_2 [mL]	0.00	52.90	16.77	0.00
$V_{100 - \Sigma (CO2 + CH4 + O2)} \approx V_{CO}$ [mL]	0.00	2867.18	2677.61	2846.07
Mass of Gas[g]	**0.00**	**7.564**	**8.231**	**11.408**
Mass of CO_2 [g]	0.00	4.191	5.117	8.078
Mass of CH_4 [g]	0.00	0.014	0.018	0.063
Mass of O_2 [g]	0.00	0.068	0.022	0.000
Mass of CO [g]	0.00	3.291	3.074	3.267
Composition of Gas [mol.%]				
Y_{CO2}	**0.00**	**0.441410**	**0.510306**	**0.603507**
Y_{CH4}	**0.00**	**0.004055**	**0.004936**	**0.012943**
Y_{O2}	**0.00**	**0.009848**	**0.003017**	**0.000000**
$Y_{100-\Sigma(CO2 + CH4 + O2)} \approx Y_{CO}$	**0.00**	**0.544687**	**0.481741**	**0.383550**

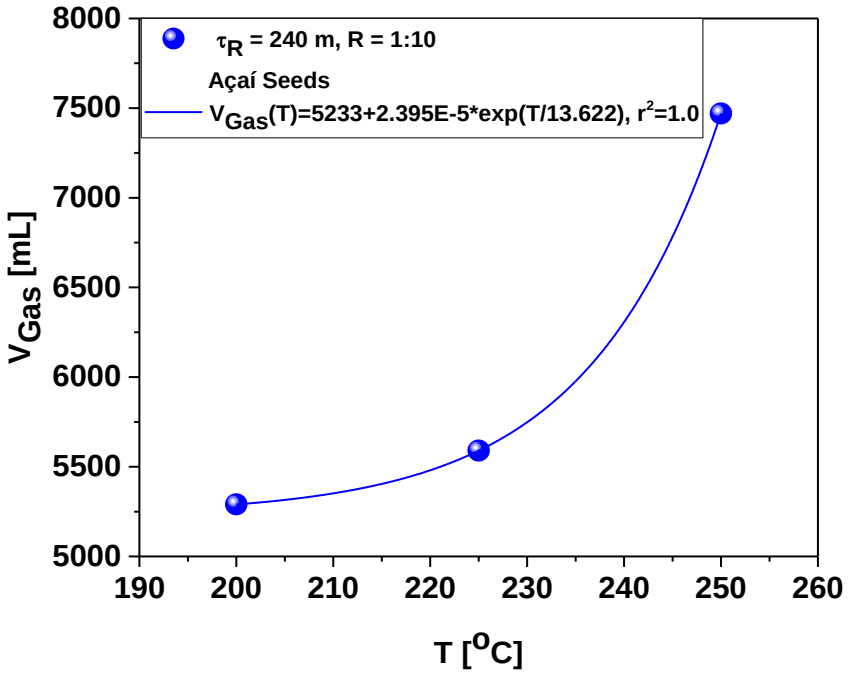

Figure 9. Effect of process temperature on the volume of gas degassed at 25 °C and 1.0 atmosphere.

Figure 9 illustrates the effect of process temperature on the volume of gas degassed at 25 °C and 1.0 atmosphere and the volumetric composition of gaseous products shown

Preprints (www.preprints.org) | NOT PEER-REVIEWED | Posted: 15 June 2021 doi:10.20944/preprints202106.0405.v1

in Figure 10. The volume of gas increases exponentially as the process temperature increases and the same behavior was reported for the hydrothermal carbonization of corn Stover by *Machado et. all.* [14]. Similar studies reported that volume of gaseous products increases with temperature [18, 31-32].

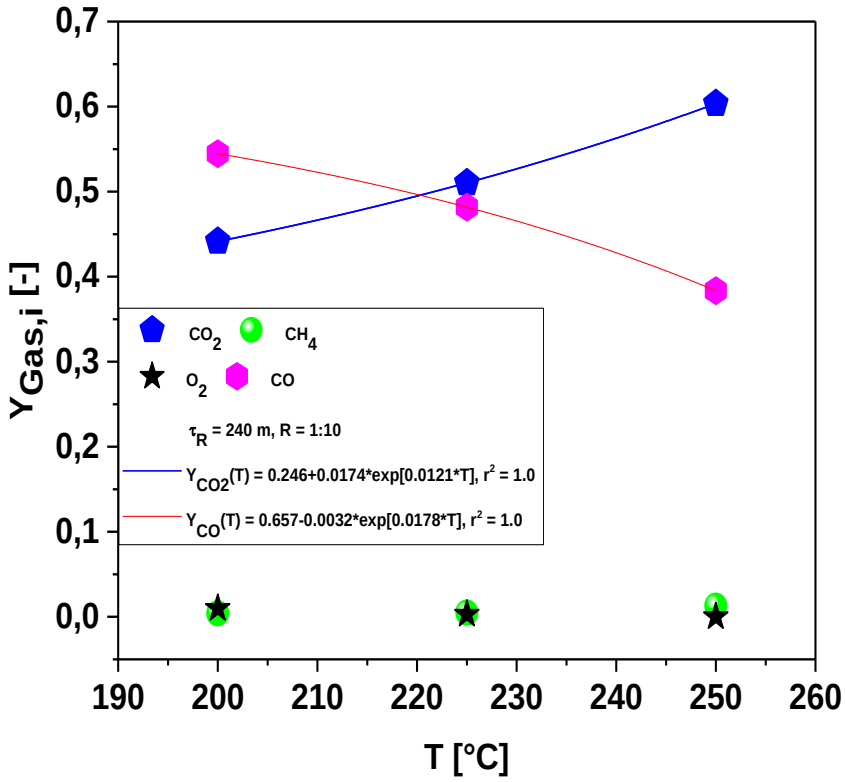

Figure 10. Effect of process temperature on the chemical composition of gas reaction products, expressed in mole fraction.

The infrared gas analyzer identified the presence of CO_2, O_2, CH_4, and CO was computed by difference [14], as summarized in Tables 5, being CO_2, the most abundant gaseous specie produced. This is according to similar studies on the evaluation of gaseous products and compositions by hydrothermal processing of biomass [14, 18, 31, 33-34]. The presence of high volumetric concentrations of CO_2 in the gaseous phase indicates that decarboxylation is probably one of the dominant reaction mechanisms/pathways by hydrothermal processing of Açaí seeds *in nature*, being according to *Li et. all.* [35]. In fact, according to the literature [36], by hydrothermal processing of biomass, decarboxylation takes place, yielding CO_2, but other sources can also produce CO_2, including de decomposition of HCOOH, produced during the hydrothermal degradation of cellulose, and until condensation reactions.

The effect of temperature on the chemical composition of gas reaction products shown in Figure 10. The mole fraction of CO shows a smooth exponential decay behavior and the mole fraction of CO_2 a smooth exponential growth. An increase on CO_2 concentration in the gaseous phase by hydrothermal processing of biomass may be explained by analogy to the mild torrefaction process of biomass, as reported by *Wannapeera et. all.* [37]. By increasing the process temperature, the oxygen functional groups in the Açaí seeds are decomposed resulting not only in higher amounts of gas formed, but also in higher yields of CO_2.

3.1.2.2. Influence of H_20-to-Biomass ratio on the volume of gas reaction products

The effect of H_20-to-Biomass ratio on the volume of gas degassed at 25 °C and 1.0 atmosphere by hydrothermal of Açaí seeds *in nature* with hot compressed H_20 at 250 °C,

Preprints (www.preprints.org) | NOT PEER-REVIEWED | Posted: 15 June 2021 doi:10.20944/preprints202106.0405.v1

2 °C/min, 240 min, and biomass-to-water ratios of 1:10, 1:15, and 1:20, in pilot scale, illustrated in Table 6 and Figure 11. By increasing the H_20-to-Biomass ratio, the volume of gas depletes, indicating that hydrolysis may be the dominant reaction mechanism [24; 38].

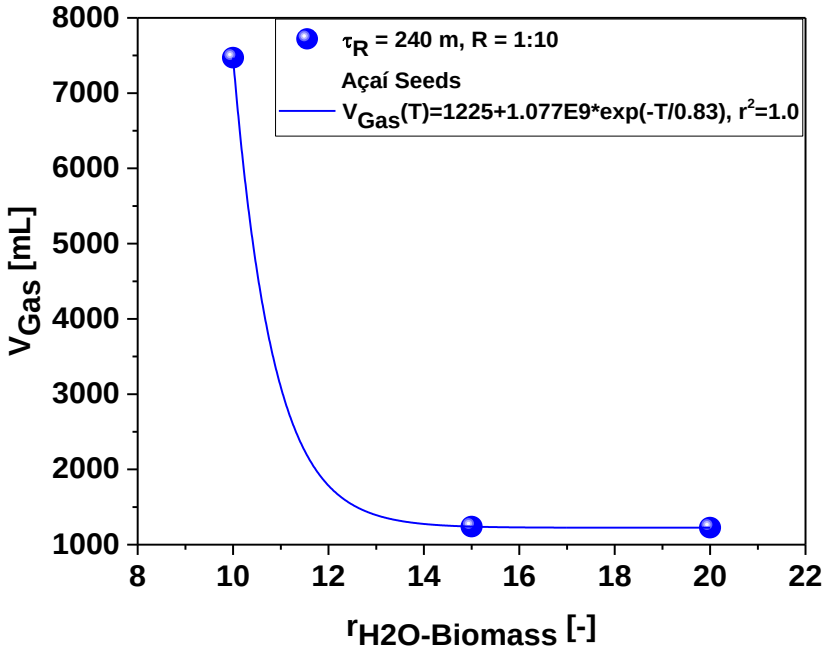

Figure 11. Effect of H20-to-Biomass on the volume of gas degassed at 25 °C and 1.0 atmosphere by hydrothermal processing of Açaí seeds with hot compressed H_20.

Table 6. Volume of gas and composition of gas products at 25 °C and 1.0 atmosphere as a function of temperature by hydrothermal processing of Açaí seeds with hot compressed H_20 at 250 °C, 2 °C/min, 240 min, and biomass-to-water ratios of 1:10, 1:15, and 1:20, in pilot scale.

	250 °C Biomass/H_2O [-]		
Composition [vol.%]	**1:10**	**1:15**	**1:20**
CO_2 [vol.%]	60.60	63.40	59.90
CH_4 [vol.%]	1.30	3.10	1.60
O_2 [vol.%]	0.00	0.00	0.00
Σ (CO_2 + CH_4 + O_2)	61.90	65.50	61.50
100 - Σ (CO_2 + CH_4 + O_2) [vol.%]	**38.10**	**33.50**	**38.50**
Volume of Gas [mL]			
Volume of CO_2 [mL]	4526.82	786.16	**733.775**
Volume of CH_4 [mL]	97.11	38.44	**19.60**
Volume of O_2 [mL]	0.00	00.00	00.00
$V_{100 - \Sigma (CO2 + CH4 + O2)} \approx V_{CO}$ **[mL]**	**2846.07**	**415.40**	**471.625**

3.1.3. Chemical composition of organic compounds in the aqueous phase

3.1.3.1. Effect of temperature on the chemical composition of organic compounds in the aqueous phase

The effect of temperature on the concentration profile of aromatic-ring compounds (Furfural, HMF, Phenols, and Cathecol) and carboxylic acids (CH_3COOH, CH_3CH_2COOH) by hydrothermal processing of Açaí seeds, illustrated in Figures 12, 13, and 14, and the data summarized in Tables 7.

Table 7. Concentration of aromatics compounds (HMF, furfural, phenol, cathecol), carboxylic acids (CH_3COOH, CH_3CH_2COOH) and total carboxylic acids (HAc) in aqueous phase at 25 °C and 1.0 atmosphere by hydrothermal processing of Açaí seeds with hot compressed H_20 at *175, 200, 225, 250* °C, 2 °C/min, 240 min, and biomass-to-water ratio of 1:10, in pilot and laboratory scales scale.

Preprints (www.preprints.org) | NOT PEER-REVIEWED | Posted: 15 June 2021 doi:10.20944/preprints202106.0405.v1

	Temperature [°C]			
	Pilot			
Concentration of aromatics [mg/L]	**175**	**200**	**225**	**250**
HMF: CAS: 67-47-0	474.8	4923	1701	24.45
Furfural: CAS:98-01-1	96.83	227.8	119.5	5.05
Phenol: CAS: 108-95-2	11.34	-	60.81	81.24
Catechol: CAS: 120-80-9	63.86	-	-	193.8
Concentration of carboxylic acids [mg/L]				
Acetic acid: CAS: 64-19-7	700	1280	1410	1680
Total acetic acid (HAc)	773.2	1394	1540	1859
Propionic Acid: CAS: 79-09-4	90	140	160	220
	Laboratory			
Concentration of aromatics [mg/L]		**200**	**225**	**250**
HMF: CAS: 67-47-0		4123	275	4.56
Furfural: CAS:98-01-1		311.5	31.82	7.28
Phenol: CAS: 108-95-2		121.2	172.5	227.99
Catechol: CAS: 120-80-9		156.84	215.4	365.61
Concentration of carboxylic acids [mg/L]				
Acetic acid: CAS: 64-19-7		3420	3690	3810
Total acetic acid (HAc)		3797	3996	4286
Propionic Acid: CAS: 79-09-4		240	310	410

Figure 12 makes a comparison for the concentration of HMF in aqueous as a function of temperature by hydrothermal processing of Açaí seeds *in nature* with hot compressed H_20 at *175, 200, 225, 250* °C, 2 °C/min, 240 min, and biomass-to-water ratio of 1:10, in laboratory and pilot scales. One observes, for the temperature interval 175-250 °C, in pilot scale, the concentration of HMF shows a Gaussian distribution. In the temperature interval 200-250 °C, the concentration of HMF decreases drastically, showing an exponential decay behavior, in both pilot and laboratory scales, being not detectable at *250* °C.

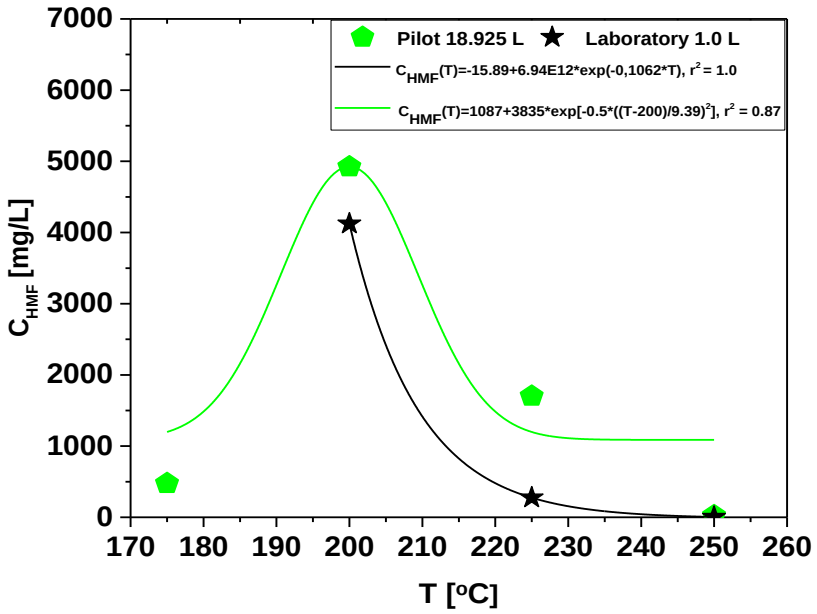

Figure 12. Effect of temperature on the concentration of HMF in the aqueous phase by hydrothermal processing of Açaí seeds *in nature*, in laboratory and pilot scales.

The concentration of HMF shows the same behavior in the temperature interval 200-250 °C, *in laboratory and pilot scales. However, there is a significant difference between concentration values, showing that production scales had a great effect on HMF concentration.*

Preprints (www.preprints.org) | NOT PEER-REVIEWED | Posted: 15 June 2021 doi:10.20944/preprints202106.0405.v1

By increasing the process temperature, the concentrations of furfural, a byproduct of cellulose degradation, decreases exponentially, in the temperature interval 200-250 °C, being present at very low concentrations at 250 °C, while the concentrations of phenols and catechol, products of furfural and HMF degradation, increase, as shown in Figure 13.

By hydrothermal processing of biomass, as cellulose hydrolyzes, it forms glucose, being transformed by isomerization reactions into fructose [38]. The decomposition of monosaccharides (glucose, fructose) produces volatile carboxylic acids, dissociating within the reaction media, thus producing hydroxonium ion (H_3O^+) and increasing the ionic product of reacting media, improving the degradation of biomass [38]. The monosaccharides (glucose, fructose) also undergo dehydration and fragmentation reaction producing furfural-derived compounds (furfural, HMF), as well as acids and aldehydes [38]. Finally, as temperature increases, furfural-derived compounds (furfural, HMF) suffer degradation, producing acids, aldehydes, and phenols [38]. In this context, based on the reaction mechanism described by Sevilla and Fuertes [38], it is expected that, by increasing the process temperature, the concentrations of Furfural and HMF will decrease, while those of cathecol and phenols increase. The results are according to similar studies reported in the literature [14, 18, 39-41]. *Jung et. all.* [42], studied the growth mechanism of hydro-char and the kinetic model of fructose degradation by hydrothermal carbonization, concluding that HMF degrades forming hydro-char and H_20 (HMF $\rightarrow$Hydro-char + H_20), following a first-order kinetics $\frac{d[Hydro-char]}{dt} = K * [HMF]$. This is according to the results for hydro-char yields in Table 1, that is, the higher the concentration of HMF, the higher the yield of hydro-char.

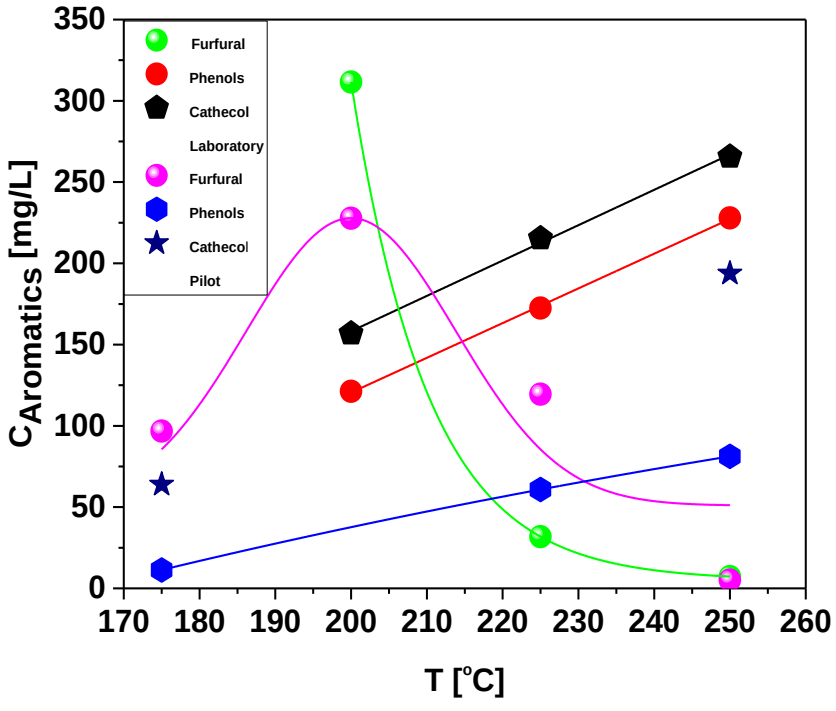

Figure 13. Effect of temperature on the concentration of aromatic compounds (Phenols, Furfural, and Cathecol).

Figure 14 shows that temperature has a great effect on concentrations of carboxylic acids (CH_3COOH, CH_3CH_2COOH) and total carboxylic acids (HAc) by hydrothermal processing of Açaí seeds with hot compressed H_20 at *175, 200, 225, 250* °C, 2 °C/min, 240 min, and biomass-to-water ratio of 1:10, in pilot scale. The concentrations of carboxylic acids, particularly CH_3COOH, the most predominant one, as well as the concentration total carboxylic acids (HAc), increase strongly with temperature. By hydrothermal processing of biomass, the monosaccharides (glucose, fructose) produced by hydrolysis of biomass are

Preprints (www.preprints.org) | NOT PEER-REVIEWED | Posted: 15 June 2021 doi:10.20944/preprints202106.0405.v1

decomposed forming volatile carboxylic acids, including acetic and propionic acids [38]. As reported by *Hoekman et. all.* [18, 43], and *Machado et. all.* [14], the concentrations of acetic acid and total organic acids produced by hydrothermal processing of different biomass feedstocks increases with temperature. *Poerschmann et. all.* [44], investigated the distribution of main medium molar mass compounds dissolved in process water by hydrothermal carbonization of glucose, fructose and xylose at 180, 220, and 250 °C by GC-MS and IC, reporting acetic acid concentrations of 4560 and 3920 for degradation of glucose and fructose, respectively, at 220 °C and 2.0 h.

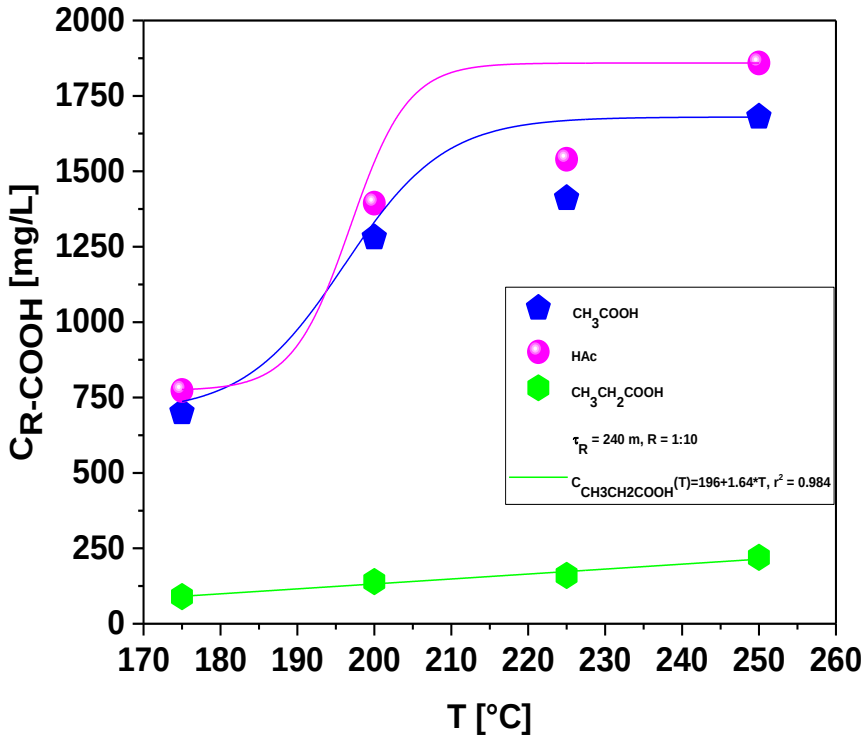

Figure 14. Effect of temperature on the concentration of carboxylic acids (CH_3COOH, CH_3CH_2COOH) and total carboxylic acids (HAc).

It is known that monosaccharides (glucose, fructose) decompose, producing not only volatile carboxylic acids, but also undergo dehydration and fragmentation reaction producing furfural-derived compounds (furfural, HMF). According to *Kabyemela et. all.* [45], the reaction mechanism/pathway of Cellobiose decomposition in sub and supercritical H_20 (300 °C/25 MPa, 350 °C/25 MPa, 350 °C/40 MPa, and 400 °C/40 MPa), fallows the sequence: hydrolysis of Cellobiose to form glucose, followed by pyrolysis to form glycosyl-erythrose and glycosyl-glycol-aldehyde, which undergo hydrolysis to produce erythrose + glucose/fructose and glycol-aldehyde + glucose/fructose, that is, glucose/fructose are intermediate-reaction products, *being produced continuously along the hydrothermal process*. However, *Hoekman et. all.* [43], reported that concentrations of glucose/xylose and total sugars decrease with increasing process temperature (215, 235, 255, 275, 295 °C) from 1.02% (wt.) to 0.08% (wt.) and 1.41% (wt.) to 0.22% (wt.), respectively, being not detected at 275 and 295 °C, such that, one may suppose that degradation of monosaccharides (glucose, fructose) are not the only reaction mechanism to produce volatile carboxylic acids by hydrothermal processing of biomass, as glucose, according to *Falco et. all.* [16], starts to be produced at 140 °C, reaching a maximum at 200 °C, where it begins to decomposes.

3.1.3.2. Effect of biomass-to-water ratio on the chemical composition of organic compounds in the aqueous phase

Preprints (www.preprints.org) | NOT PEER-REVIEWED | Posted: 15 June 2021 doi:10.20944/preprints202106.0405.v1

The effect of biomass-to-water ratio on the concentration profile of aromatic-ring compounds (Furfural, HMF, Phenols, and Cathecol) and carboxylic acids (CH_3COOH, CH_3CH_2COOH) by hydrothermal processing of Açaí seeds, illustrated in Figure 15 and 16, and the data summarized in Table 8.

Table 8. Concentration of aromatics compounds (HMF, furfural, phenol, cathecol), carboxylic acids (CH_3COOH, CH_3CH_2COOH) and total carboxylic acids (HAc) in aqueous phase at 25 °C and 1.0 atmosphere by hydrothermal processing of Açaí seeds with hot compressed H_20 at *175, 200, 225, 250* °C, 2 °C/min, 240 min, and biomass-to-water ratio of 1:10, in pilot scale.

	250 °C Biomass/H_20 [-]		
Concentration of aromatics [mg/L]	**1:10**	**1:15**	**1:20**
HMF: CAS: 67-47-0	24.450	5.188	3.002
Furfural: CAS:98-01-1	5.054	2.972	2.194
Phenol: CAS: 108-95-2	81.24	81.78	89.33
Catechol: CAS: 120-80-9	195.6	193.8	185.9
Concentration of carboxylic acids [mg/L]			
Acetic acid: CAS: 64-19-7	1680	1270	1070
Total acetic acid (HAc)	1859	1424	1070
Propionic Acid: CAS: 79-09-4	220	190	20

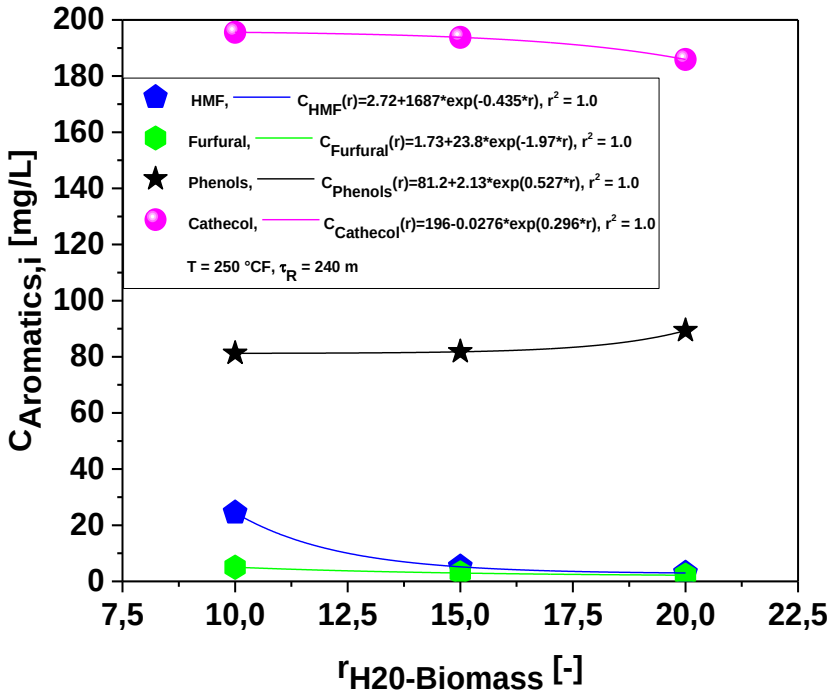

Figure 15. Effect of H_20-to-Biomass ratio on the concentration of aromatic (Phenols, Furfural, HMF, and Cathecol).

By increasing the H_20-to-Biomass ratio, the concentrations of furfural and HMF are very low and decrease smoothly, while that of phenols shows a smooth first-order exponential growth behavior, as shown in Figure 15. In addition, the carboxylic acids (CH_3COOH, CH_3CH_2COOH) and total carboxylic acids (HAc) also decrease as the H_20-to-Biomass ratio increases, illustrated in Figure 16.

In a first look, Figures 15 and 16 do not say much, as the concentration was measured in mg/L, so that, increasing the H_20-to-Biomass ratio, the volume of reaction media increases, and hence it is to expect a decrease on the concentration of main organic compounds dissolved in process water, but performing a mass balance by multiplying the concentration of main organic compounds dissolved in process water, described in Table 8, and the volume of process water (Mass of Liquid Phase + Σ Process Loss + Mass of Moist

Preprints (www.preprints.org) | NOT PEER-REVIEWED | Posted: 15 June 2021 doi:10.20944/preprints202106.0405.v1

Hydro-char - Mass of Dry Hydro-char - Mass of Gas), described in Table 3, it can be shown that increasing the H_20-to-Biomass ratio has caused an increase on the mass production of chemicals, as shown in Figures 17 and 18.

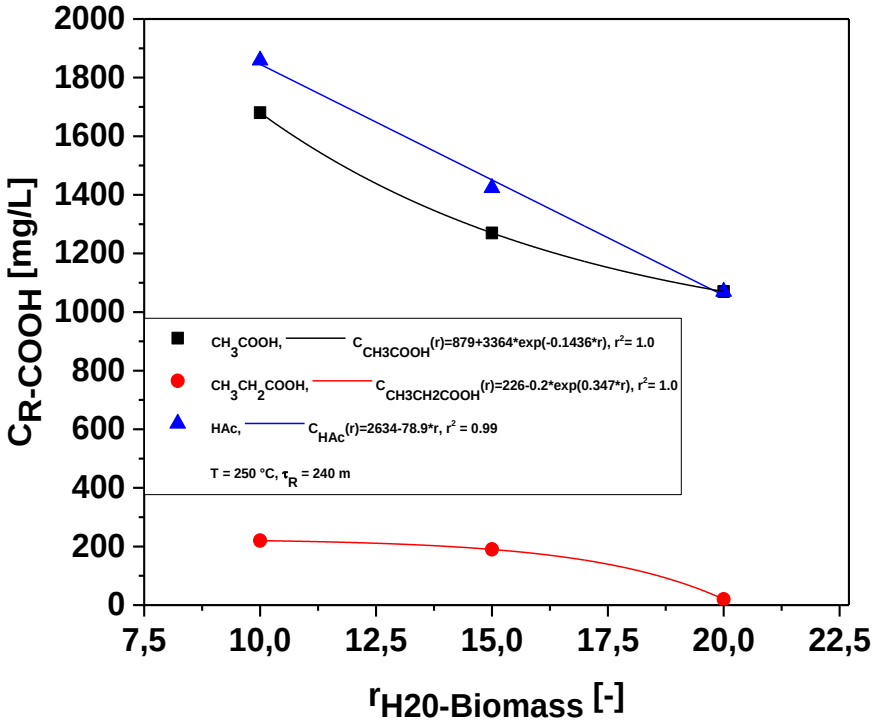

Figure 16. Effect of H_20-to-Biomass ratio on the concentration of carboxylic acids (CH_3COOH, CH_3CH_2COOH) and total carboxylic acids (HAc).

According to the literature [24-25], increasing the H_20-to-Biomass ratio causes a great impact on hydrolysis reactions by hydrothermal processing of biomass, so that, the remaining cellulose in biomass is hydrolyzed, producing monosaccharides (glucose, fructose), and the decomposition of monosaccharides (glucose, fructose) produces volatile carboxylic acids, particularly acetic acid, confirmed by Figure 17.

It may be concluded that hydrolysis is probably the dominant reaction mechanism, but not the only one, by hydrothermal processing of Açaí seeds with hot compressed H_20 at *250* °C, 2 °C/min, 240 min, as biomass-to-water ratio increase from 1:10 to 1:20.

Preprints (www.preprints.org) | NOT PEER-REVIEWED | Posted: 15 June 2021 doi:10.20944/preprints202106.0405.v1

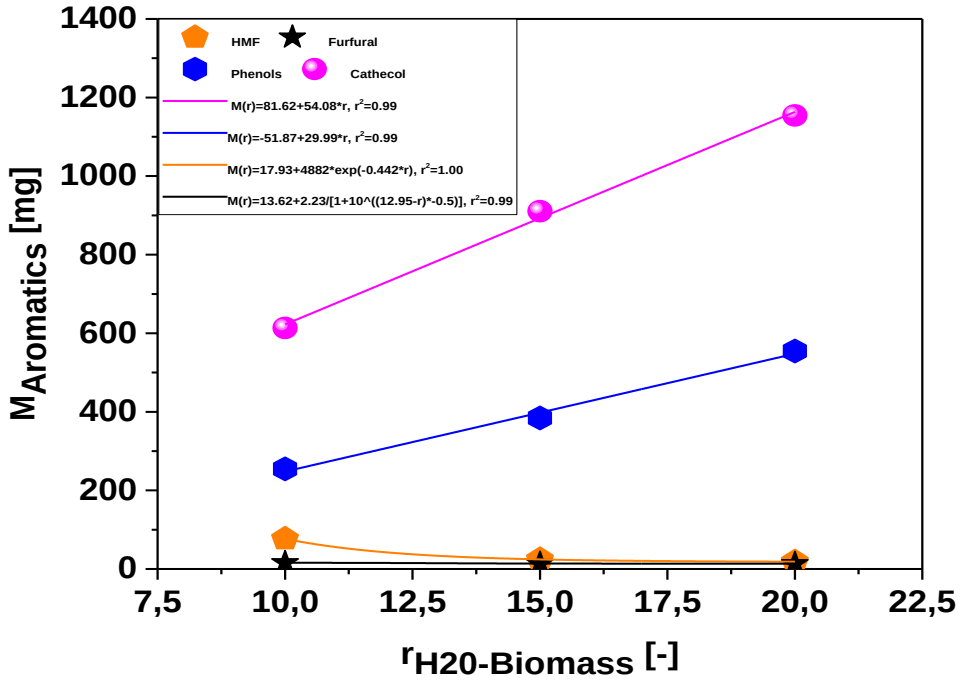

Figure 17. Effect of H_20-to-Biomass ratio on the on the mass production of acetic acid (CH_3COOH).

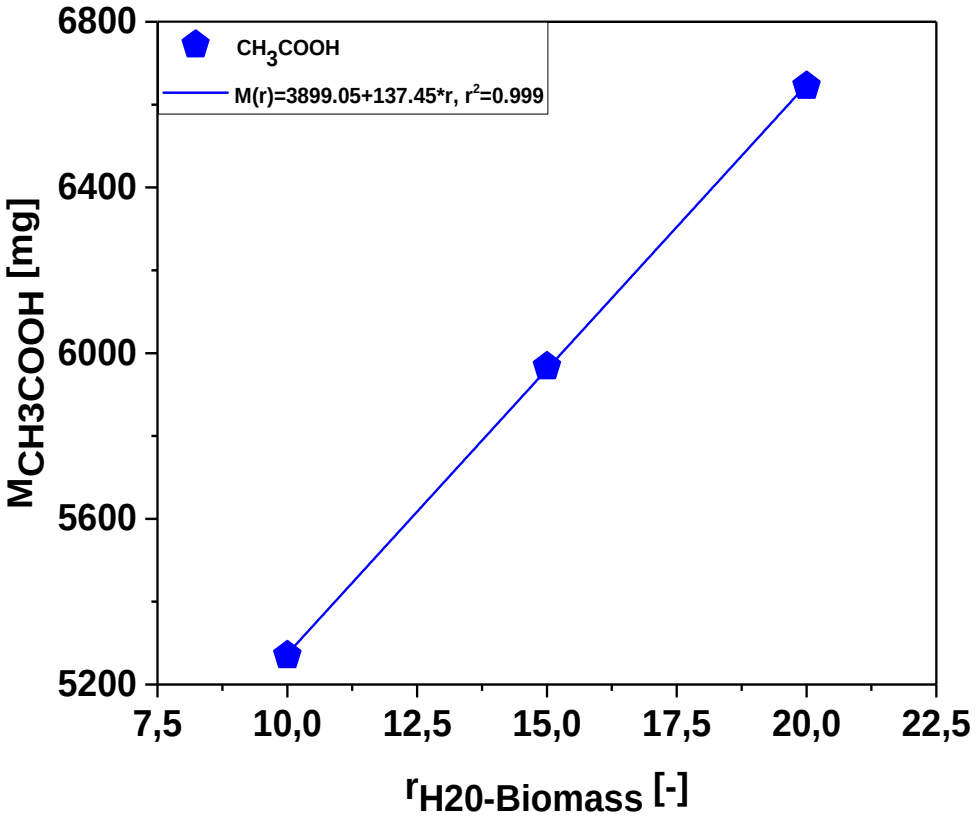

Figure 18. Effect of H_20-to-Biomass ratio on the on the mass production of aromatic compounds (Phenols, Cathecol).

 doi:10.20944/preprints202106.0405.v1

5. Conclusions

The yield of solids shows a smooth first-order exponential decay behavior, while that of liquid and gaseous phases a smooth first-order exponential growth. At 175 °C hydrothermal carbonization takes places, as the main reaction product is a solid [15]. From 200 °C, hydrothermal liquefaction occurs, as the maim reaction products are liquids [15].

Based on the centesimal composition of Açaí (*Euterpe oleracea* Mart.) seeds [12], one may perform a centesimal mass balance to compute the approximate theoretical mass degradation of Açaí seeds at 200 °C, 2 °C/min, 240 min, and biomass-to-water ratio of 1:10, obtaining for the solid phase yield 41.01% (wt.), very close to the experimental value of 39.534% (wt.), showing a deviation of 3.73%.

The yields of hydro-char and gas decrease with H_20-to-water ratios, while that of liquid phase increases. Increasing the H_20-to-Biomass ratio causes a great impact on hydrolysis reactions by hydrothermal processing of biomass.

The presence of high volumetric concentrations of CO_2 in the gaseous phase indicates that decarboxylation is probably one of the dominant reaction mechanisms/pathways by hydrothermal processing of Açaí seeds *in nature*, being according to *Li et. all.* [35].

The concentrations of furfural and HMF, decreases exponentially, being present at very low concentrations at 250 °C, as temperature increases, while the concentrations of phenols and cathecol increase.

By increasing the H_20-to-Biomass ratio, the concentrations of furfural and HMF are very low and decrease smoothly, while that of phenols shows a smooth first-order exponential growth behavior. In addition, the carboxylic acids (CH_3COOH, CH_3CH_2COOH) and total carboxylic acids (HAc) also decrease as the H_20-to-Biomass ratio increases. Performing a mass balance, it can be shown that increasing the H_20-to-Biomass ratio has caused an increase on the mass production of chemicals, particularly acetic acid.

It may be concluded that hydrolysis is probably the dominant reaction mechanism, but not the only one, by hydrothermal processing of Açaí seeds with hot compressed H_20 at *250* °C, 2 °C/min, 240 min, as biomass-to-water ratio increase from 1:10 to 1:20.

Supplementary Materials: The following are available online at www.mdpi.com/xxx/s1, Table S1: Centesimal and elemental characterization of Açaií (*Euterpe oleracea*, Mart) seeds in *nature*, compared to similar studies reported in the literature [1-4].

Author Contributions: The individual contributions of all the co-authors are provided as follows: Conceição de Maria Sales da Silva contributed with *formal analysis and writing—original draft preparation*, Douglas Alberto Rocha de Castro contributed with *formal analysis and writing—original draft preparation*, Marcelo Costa Santo contributed with *formal analysis and software*, Hélio da Silva Almeida contributed with *formal analysis, software, and visualization*, Ulf Lüder contributed with *investigation and validation*, Maja Shultze contributed with *investigation and methodology*, Judi A. Libra with *funding acquisition*, Jan Mumme contributed with *funding acquisition*, Thomas Hofmann contributed with *resources and project administration*, and Nélio Teixeira Machado contributed with *supervision, conceptualization,* and *data curation*. *All authors have read and agreed to the published version of the manuscript*.

Funding: This research was partially funded by CNPq-Brazil, grant number: 207325/2014-6.

Acknowledgments: I would like to acknowledge the Department of Postharvest Technology at Leibnitz-Institüt für Agrartechnik Potsdam-Bornin e.V, for the opportunity to research at the Laboratory of Biochar, as well as for providing all the technical support (administrative, infra-structure, analytics) and materials to develop this research.

Conflicts of Interest: The authors declare no conflict of interest.

References

1. Marcelo Morita Lindolfo; Gilson Sérgio Bastos de Matos; Wendel Valter da Silveira Pereira; Antônio Rodrigues Fernandes. Productivity and nutrition of fertigated açaí palms according to boron fertilization. Rev. Bras. Frutic. vol.42 nº.2 Jaboticabal 2020 Epub Apr 06, 2020; https://doi.org/10.1590/0100-29452020601
2. Michael Heinrich; Tasleem Dhanji; Ivan Casselman. Açai (Euterpe oleracea. Mart.)—A phytochemical and pharmacologicalassessment of the species' health claims. Phytochemistry Letters 4 (2011) 10–2111
3. Sara Sabbe; Wim Verbeke; Rosires Deliza; Virginia Matta; Patrick Van Damme. Effect of a health claim and personal characteristics on consumer acceptance offruit juices with different concentrations of açaí (Euterpe oleraceaMart.). Appetite 53 (2009) 84–9286
4. David del Pozo-Insfran; Carmen H. Brenes; Stephen T. Talcott. Phytochemical Composition and Pigment Stability of Açai (*Euterpe oleracea* Mart.). J. Agric. Food Chem. 2004, 52, 1539−1545
5. José Dalton Cruz Pessoa; Paula Vanessa da Silva e Silva. Effect of temperature and storage on açaí (Euterpe oleracea) fruit water uptake: simulation of fruit transportation and pre-processing. Fruits, 2007, Vol. 62, 295–302; DOI: 10.1051/fruits:2007025
6. D. R. Pompeu; E. M. Silva; H. Rogez. Optimisation of the solvent extraction of phenolic antioxidants from fruits of Euterpe oleracea using Response Surface Methodology. Bioresource Technology 100 (2009) 6076–6082
7. Felipe Fernando da Costa Tavares; Marcos Danilo Costa de Almeida; João Antônio Pessoa da Silva; Ludmila Leite Araújo; Nilo Sérgio Medeiros Cardozo; Ruth Marlene Campomanes Santana. Thermal treatment of açaí (*Euterpe oleracea*) fiber for composite reinforcement. Polímeros vol.30 n°.1 São Carlos 2020 Epub July 01, 2020
8. Lina Bufalino; Arqueanise Andrade Guimaraes; Breno Marques da Silva e Silva; Rafael Lucas Figueiredo de Souza; Isabel Cristina Nogueira Alves de Melo; Dhimitrius Neves Paraguassu Smith de Oliveira; Paulo Fernando Trugilho. Local variability of yield and physical properties of açaí waste and improvement of its energetic attributes by separation of lignocellulosic fibers and seeds. J. Renewable Sustainable Energy 10, 053102 (2018)
9. Anna Cristina Pinheiro de Lima; Dandara Leal Ribeiro Bastos; Mariella Alzamora Camarena; Elba Pinto Silva Bom; Magali Christe Cammarota; Ricardo Sposina Sobral Teixeira; Melissa Limoeiro Estrada Gutarra. Physicochemical characterization of residual biomass (seed and fiber) from açaí (Euterpe oleracea) processing and assessment of the potential for energy production and bioproducts. Biomass Conversion and Biorefinery, https://doi.org/10.1007/s13399-019-00551-w
10. José Dalton Cruz Pessoa; Marcos Arduin; Maria Alice Martins; José Edmar Urano de Carvalho. Characterization of açaí (*E. oleracea*) fruits and its processing residues. Braz. arch. biol. technol. vol.53 no.6 Curitiba Nov./Dec. 2010, https://doi.org/10.1590/S1516-89132010000600022
11. Andrezza de Melo Barbosa; Viviane Siqueira Magalhães Rebelo; Lucieta Guerreiro Martorano; Virginia Mansanares Giacon. Characterization of acai waste particles for civil construction use. Revista Matéria, v.24, n.3, 2019, http://dx.doi.org/10.1590/s1517-707620190003.0750
12. D. A. R. de Castro; H. J. da Silva Ribeiro; C. C. Ferreira; L. H. H. Guerreiro; M. de Andrade Cordeiro; A. M. Pereira; W. G. dos Santos; F. B. de Carvalho; J. O. C. Silva Jr.; R. Lopes e Oliveira; M. C. Santos; S. Duvoisin Jr; L. E. P. Borges; N. T. Machado. Fractional Distillation of Bio-Oil Produced by Pyrolysis of Açaí (Euterpe oleracea) Seeds. Fractionation, Editor Hassan Al-Haj Ibrahim: Fractionation, Intechopen ISBN: 978-1-78984-965-3, DOI: 10.5772/intechopen.79546
13. Liang Li; Joseph R. V. Flora; Juan M. Caicedo; Nicole D. Berge. Investigating the role of feedstock properties and process conditions on products formed during the hydrothermal carbonization of organics using regression techniques. Bioresource Technology 187 (2015) 263–274
14. N. T. Machado; D. A. R. de Castro; M. C. Santos; M. E. Araújo; U. Lüderf; L. Herklotz; M. Werner; J. Mumme; T. Hoffmann. Process analysis of hydrothermal carbonization of corn Stover with subcritical H_2O. The Journal of Supercritical Fluids 136 (2018) 110–122
15. M. Möller; P. Nilges; F. Harnisch; U. Schröder. Subcritical water as reaction environment: fundamentals of hydrothermal biomass transformation, ChemSusChem4 (2011) 566–579, http://dx.doi.org/10.1002/cssc.201000341
16. Camillo Falco; Niki Baccile; Maria-Magdalena Titirici. Morphological and structural differences between glucose, cellulose and lignocellulosic biomass derived hydrothermal carbons. Green Chem., 2011, 13, 3273
17. Zhengang Liu; R. Balasubramanian. Hydrothermal carbonization of waste biomass for energy generation Procedia Environmental Sciences 16 (2012) 159 – 166
18. S. Kent Hoekman; Amber Broch; Curtis Robbins; Barbara Zielinska; Larry Felix. Hydrothermal carbonization (HTC) of selected woody and herbaceous biomass feedstocks. Biomass Conv. Bioref. (2013) 3:113–126
19. Shuqing Guo; Xiangyuan Dong; Tingting Wu; Caixia Zhu. Influence of reaction conditions and feedstock on hydrochar properties. Energy Conversion and Management 123 (2016) 95–103
20. Gule Teri; Ligang Luo; Phillip E. Savage. Hydrothermal Treatment of Protein, Polysaccharide, and Lipids Alone and in Mixtures. Energy Fuels 2014, 28, 7501−7509
21. A. M. Borrero-López; E. Masson; A. Celzard; V. Fierro. Modelling the reactions of cellulose, hemicellulose and lignin submitted to hydrothermal treatment. Industrial Crops & Products 124 (2018) 919–930
22. Yongfang Zhang; Wensheng Hou; Hong Guo; Sheng Shi; Jinming Dai. Preparation and Characterization of Carbon Microspheres From Waste Cotton Textiles By Hydrothermal Carbonization. JRM, 2019, vol.7, n°.12, DOI: 10.32604/jrm.2019.07884
23. Ilker Örtürk; Sibel Irmak; Arif Hesenov; Oktay Erbatur. Hydrolysis of kenaf (Hibiscus cannabinus L.) stems by catalytical thermal treatment in subcritical water. Biomass and Bioenergy 34 (2010) 1578-1585

24. S. Román; J.M.V. Nabais; C. Laginhas; B. Ledesma; J.F. González. Hydrothermal carbonization as an effective way of densifying the energy content of biomass. Fuel Processing Technology 103 (2012) 78–83
25. Ekaterina Sermyagina; Jussi Saari; Juha Kaikko; Esa Vakkilainen. Hydrothermal carbonization of coniferous biomass: Effect of process parameters on mass and energy yields. Journal of Analytical and Applied Pyrolysis 113 (2015) 551–556
26. E. Sabio; A. Álvarez-Murillo; S. Román; B. Ledesma. Conversion of tomato-peel waste into solid fuel by hydrothermal carbonization: Influence of the processing variables. Waste Management 47 (2016) 122–132
27. A. Álvarez-Murillo; S. Román; B. Ledesma; E. Sabio. Study of variables in energy densification of olive stone by hydrothermal carbonization. Journal of Analytical and Applied Pyrolysis 113 (2015) 307–314
28. Steven M. Heilmann; H. Ted Davis; Lindsey R. Jader; Paul A. Lefebvre; Michael J. Sadowsky; Frederick J. Schendel; Marc G. von Keitz; Kenneth J. Valentas. Hydrothermal carbonization of microalgae. Biomass and Bioenergy 34 (2010) 875–882
29. Cyrilla Oktaviananda; Ria F. Rahmawati; Agus Prasetya; Chandra W. Purnomo; Ahmad T. Yuliansyah; Rochim B. Cahyono. Effect of Temperature and Biomass-Water Ratio to Yield and Product Characteristics of Hydrothermal Treatment of Biomass. AIP Conference Proceedings 1823, 020029 (2017); https://doi.org/10.1063/1.4978102
30. Herlian Eriska Putra; Enri Damanhuri; Kania Dewi; Ari Darmawan Pasek. Hydrothermal carbonization of biomass waste under low temperature condition. MATEC Web of Conferences 154, 01025 (2018), https://doi.org/10.1051/matecconf/201815401025
31. Daniele Castello; Andrea Kruse; Luca Fiori. Biomass gasification in supercritical and subcritical water: The effect of the reactor material. Chemical Engineering Journal 228 (2013) 535–544
32. Michela Lucian; Luca Fiori. Hydrothermal carbonization of waste biomass: process design, modeling, energy efficiency and cost analysis, Energies 10 (211) (2017)1–18
33. Funke Axel, Reebs Felix, Kruse Andrea. Experimental comparison of hydrothermal and vapothermal carbonization. Fuel Process. Technol. 115 (2013) 261–269
34. Zhang, H.J. Huang, S. Ramaswamy, Reaction kinetics of the hydrothermal treatment of lignin. Appl. Biochem. Biotechnol. 147 (2008) 119–131
35. Liang Li; Ryan Diederick; Joseph R. V. Flora; Nicole D. Berge. Hydrothermal carbonization of food waste and associated packaging materials for energy source generation. Waste Management 33 (2013) 2478–2492
36. Axel Funke; Felix Ziegler. Hydrothermal carbonization of biomass: A summary and discussion of chemical mechanisms for process engineering. *Biofuels, Bioprod. Bioref*. 4:160–177 (2010)
37. Janewit Wannapeera; Bundit Fungtammsan; Nakorn Worasuwannarak. Effects of temperature and holding time during torrefaction on the pyrolysis behaviors of woody biomass. Journal of Analytical and Applied Pyrolysis 92 (2011) 99–105
38. M. Sevilla; A. B. Fuertes. The production of carbon materials by hydrothermal carbonization of cellulose. CARBON 47 (2009) 2281–2289
39. Roland Becker; Ute Dorgerloh; Ellen Paulke; Jan Mumme; Irene Nehls. Hydrothermal Carbonization of Biomass: Major Organic Components of the Aqueous Phase. Chem. Eng. Technol. 2014, 37, No. 3, 511–518
40. M. Toufiq Reza; Benjamin Wirth; Ulf Lüder; Maja Werner. Behavior of selected hydrolyzed and dehydrated products during hydrothermal carbonization of biomass. Bioresource Technology 169 (2014) 352–361
41. Roland Becker; Ute Dorgerloh; Mario Helmis; Jan Mumme; Mamadou Diakité; Irene Nehl. Hydrothermally carbonized plant materials: Patterns of volatile organic compounds detected by gas chromatography. Bioresource Technology 130 (2013) 621–628
42. Dennis Jung; Michael Zimmermann; Andrea Kruse. Hydrothermal Carbonization of Fructose: Growth Mechanism and Kinetic Model. ACS Sustainable Chem. Eng. 2018, 6, 13877−13887
43. Hoekman, S.K.; Broch, A.; Robbins, C. Hydrothermal carbonization (HTC) of lignocellulosic biomass. Energy Fuels 25(4), 1802–1810 (2011)
44. Juergen Poerschmann; Barbara Weiner; Robert Koehler; Frank-Dieter Kopinke. Hydrothermal Carbonization of Glucose, Fructose, and Xylose-Identification of Organic Products with Medium Molecular Masses. ACS Sustainable Chem. Eng. 2017, 5, 6420−6428
45. B. M. Kabyemela; M. Takigawa; T. Adschiri; R. M. Malaluan; and K. Arai. Mechanism and Kinetics of Cellobiose Decomposition in Sub- and Supercritical Water. Ind. Eng. Chem. Res. 1998, 37, 357-361
46. Silvia Román; Judy Libra; Nicole Berge; Eduardo Sabio; Kyoung Ro; Liang Li; Beatriz Ledesma; Andrés Álvarez; Sunyoung Bae. Hydrothermal Carbonization: Modeling, Final Properties Design and Applications: A Review. Energies 2018, 11, 216; doi:10.3390/en11010216
47. Johnatt A. R. Oliveira; Andrea Komesu; Rubens Maciel Filho. Hydrothermal Pretreatment for Enhancing Enzymatic Hydrolysis of Seeds of Açaí (Euterpe oleracea) and Sugar Recovery. CHEMICAL ENGINEERING TRANSACTIONS VOL. 37, 2014, 785-792
48. Standards T. Acid-Insoluble Lignin in Wood and Pulp. Tappi Method T 222 Om-06. Atlanta, GA: Tappi Press. 2006
49. Buffiere P; Loisel D. Dosage des fibres Van Soest. Weened, Laboratoire de Biotechnologie de l'Environnement. INRA Narbonne. 2007:1-14